organoids

MDPI

Article

Pre-Adipocytes in 3D Co-Culture Underwent Self-Differentiation: New Perspectives for an Old Model

Tamara Dal-Mora [1], Najla Adel Saleh [1], Veridiana Pacheco Goulart Martinazzo [1], Maria Luiza Carneiro Buchele [1], Michele Patrícia Rode [1], Adny Henrique Silva [1], Laura Sartori Assunção [1], Tânia Beatriz Creczynski-Pasa [2] and Fabiola Branco Filippin-Monteiro [3,*]

[1] Programa de Pós-Graduação em Farmácia, Centro de Ciências da Saúde, Universidade Federal de Santa Catarina, Florianópolis 88040900, SC, Brazil; tamaradalmora@hotmail.com (T.D.-M.); najladelsaleh@gmail.com (N.A.S.); veridianamartinazzo@gmail.com (V.P.G.M.); buchelemalu@gmail.com (M.L.C.B.); mip.rode@gmail.com (M.P.R.); adnyhe@gmail.com (A.H.S.); laura_sartori22@hotmail.com (L.S.A.)

[2] Departamento de Ciências Farmacêuticas, Centro de Ciências da Saúde, Universidade Federal de Santa Catarina, Florianópolis 88040900, SC, Brazil; tania.pasa@ufsc.br

[3] Departamento de Análises Clínicas, Centro de Ciências da Saúde, Universidade Federal de Santa Catarina, Florianópolis 88040900, SC, Brazil

* Correspondence: fabiola.monteiro@ufsc.br

Abstract: Adipogenesis is a complex process influenced by various cellular interactions within adipose tissue, which plays a critical role in metabolic homeostasis. This study aimed to develop a novel in vitro three-dimensional (3D) co-culture model using murine 3T3-L1 pre-adipocytes, J774 macrophages, and NIH-3T3 fibroblasts to investigate adipogenic differentiation and inflammatory pathways. We first validated an adipogenic differentiation protocol in a two-dimensional (2D) model, where 3T3-L1 pre-adipocytes were subjected to a hormonal medium containing 3-isobutyl-1-methylxanthine, dexamethasone and insulin. After 7 days, differentiated cells were analyzed using Oil Red O and Nile Red staining, confirming lipid accumulation. Subsequently, spheroids were formed in 3D cultures, with monospheroids and heterospheroids maintained in either control medium or MDI for 11 days. Size measurements indicated significant growth in heterospheroids, particularly in the 3T3-L1:J774 combination, underscoring the importance of cellular interactions. Confocal microscopy and flow cytometry analyses demonstrated that even in the absence of hormonal stimuli, control spheroids exhibited adipogenic differentiation, evidenced by a notable proportion of Nile Red-positive cells (75.7 $\pm$ 1.7%). Inflammatory profiling revealed that the heterospheroid 3:J produced the highest levels of nitric oxide (NO), with no significant differences observed between control and MDI conditions. This study highlights the potential of 3D co-culture systems for elucidating the intricate interactions among adipocytes, macrophages, and fibroblasts. The findings may provide valuable insights into novel therapeutic targets for metabolic disorders.

Keywords: obesity; adipose tissue; 3D culture; spheroid model; adipogenic differentiation; adipose inflammation

Citation: Dal-Mora, T.; Saleh, N.A.; Martinazzo, V.P.G.; Buchele, M.L.C.; Rode, M.P.; Silva, A.H.; Assunção, L.S.; Creczynski-Pasa, T.B.; Filippin-Monteiro, F.B. Pre-Adipocytes in 3D Co-Culture Underwent Self-Differentiation: New Perspectives for an Old Model. *Organoids* **2024**, *3*, 295–308. https://doi.org/10.3390/organoids3040018

Academic Editor: Holm Zaehres

Received: 17 October 2024
Revised: 4 December 2024
Accepted: 11 December 2024
Published: 18 December 2024

1. Introduction

Considered the most significant nutritional disorder, obesity has become a major public health concern, responsible for 2.8 million deaths annually worldwide, according to the World Health Organization [1]. Obesity is characterized by an excessive accumulation of white adipose tissue (WAT), resulting from an imbalance between energy intake and expenditure. This accumulation is often accompanied by mild or chronic systemic inflammation [2]. Consequently, obesity significantly increases the risk of developing type 2 diabetes, cardiovascular diseases, and certain types of cancer [3]. The rising prevalence of

obesity has sparked growing interest in studying adipose tissue biology, as well as gaining a deeper understanding of its cellular and molecular mechanisms [4].

In addition to fat storage, adipose tissue is known to secrete a wide range of adipokines that regulate systemic energy homeostasis through autocrine, paracrine, or endocrine mechanisms, protecting various tissues from lipotoxicity and metabolic dysfunctions. Adipokines, including leptin, adiponectin, and others, play key roles in regulating metabolism, appetite, cardiovascular function, and several physiological processes. Therefore, adipose tissue is not merely a repository of adipocytes but also an integral part of the body's endocrine system [5,6].

Adipocytes are the primary cellular component of WAT, essential for both energy storage and endocrine activity. In addition to adipocytes, WAT is composed of mesenchymal cells, preadipocytes (precursor cells), macrophages, T cells, fibroblasts, vascular cells (endothelial and vascular smooth muscle cells), extracellular matrix, blood vessels, and capillaries [7].

Adipogenic differentiation, or adipogenesis, occurs throughout life as part of normal cell turnover and in response to increased fat storage demands [8]. This process can lead to rapid tissue remodeling through adipocyte hypertrophy and hyperplasia [9]. Conversely, when caloric intake is insufficient and energy expenditure is elevated, WAT releases stored components into the bloodstream, where they are transported to other tissues and oxidized to produce energy [10]. Adipogenesis is the transformation of preadipocytes into adipocytes, a multi-phase process that involves the activation of several transcription factors, including C/EBPα and PPARγ, which are essential for the differentiation of precursor cells into mature adipocytes. The expression patterns of key transcripts and proteins are tightly coordinated throughout the stages of adipogenesis [11]. These critical regulators of adipocyte differentiation include fatty acid binding protein 4 (FABP4), adiponectin, IL-6, leptin, glucose transporter type 4 (GLUT4), cluster of differentiation 36 (CD36), and insulin receptor substrate 1 (IRS1) [12].

Molecular and cellular mechanisms involved in the adipogenesis process have been extensively studied using various in vitro model systems [13–16]. The 3T3-L1 cell line (preadipocytes), first described by [17], has become a well-established in vitro model for studying adipogenesis. Despite their morphological similarity, these cells are already committed to the adipocyte lineage. When treated with a hormonal medium containing fetal bovine serum, isobutylmethylxanthine, dexamethasone, and insulin, 3T3-L1 cells undergo differentiation into mature adipocytes. This process is characterized by a change in morphology to a spherical shape, lipid accumulation, and the expression of fat differentiation markers [18,19].

Obesity models using 3T3-L1 cells have been developed to evaluate the activity of new compounds with therapeutic potential for obesity treatment, particularly those that inhibit adipogenesis and reduce inflammatory adipokines [20–22]. In addition, the relationship between obesity and diseases such as cancer and diabetes has been studied using the 3T3-L1 cell line [13,23,24]. The role of various genes involved in adipogenesis has also been investigated through gene silencing techniques [25–27]. Furthermore, studies have utilized 3T3-L1 cells to explore the role of miRNAs as mediators of preadipocyte differentiation into adipocytes, focusing on their regulation of genes involved in the cell cycle [28–30].

Co-culture systems combining adipocytes with other cell types, such as macrophages and fibroblasts, are crucial for studying inflammatory pathways, adipokine synthesis, and release, as well as for understanding the complex interactions between adipose tissue and other tissues in the body [31,32]. Reproducing these cellular interactions in vitro offers a valuable strategy for investigating and comprehending cell–cell dynamics involved in the progression of various diseases.

Three-dimensional cell culture systems integrate different cell types into a specialized environment that forms a three-dimensional structure, closely mimicking the natural tissue architecture. These models have shown great potential for more accurately simulating the in vivo microenvironment, providing a more physiologically relevant system for studying

complex tissue behaviors [33–35]. Additionally, 3D systems facilitate the examination of cellular and molecular interactions, changes in the extracellular matrix, and signaling pathways. Unlike traditional 2D cultures, cells in 3D environments, particularly in co-culture systems, more effectively replicate the in vivo tissue architecture, enhancing the relevance of experimental findings.

In this study, we used murine, immortalized cell lines—pre-adipocytes, fibroblasts, and macrophages—chosen for their ease of acquisition, cultivation, and ability to reliably replicate in vitro adipose tissue interactions. Pre-adipocytes are the progenitors of adipocytes, while fibroblasts provide structural integrity and contribute to adipose tissue plasticity, supporting adipogenic differentiation. Macrophages are crucial for immune response and tissue remodeling, adding an inflammatory component to the adipose tissue microenvironment. The inclusion of these cell types enables a more comprehensive representation of adipose tissue interactions, reflecting its natural complexity. These cells are co-cultured in a 3D system, promoting cell–cell aggregation and spheroid formation, with agarose hydrogels providing a non-adherent surface to facilitate spheroid assembly. This versatile material supports the growth of various cell types and is essential for developing an effective, in vitro adipose tissue model. Agarose hydrogels, used in the liquid-overlay method, promote cell–cell aggregation and spheroid formation. This material is versatile, allowing its use with various cell types. Additionally, the extracellular matrix and microenvironment in adipose tissue exhibit significant complexity due to interactions between adipocytes, preadipocytes, stromal cells, endothelial cells, and immune cells [36–40].

In the context of obesity, spheroid models developed thus far using 3T3-L1 pre-adipocytes have primarily focused on studying adipogenic processes, adipocyte functions, and pro-inflammatory pathways, making them a valuable platform for investigating the adipose tissue microenvironment [35,41–44]. However, most current models rely on cells derived from human adipose tissue, which can be difficult to obtain and cultivate. In contrast, the model developed in this study incorporates murine pre-adipocytes, macrophages, and fibroblasts, all of which are immortalized cell lines that are easy to obtain and culture. The primary objective of this study was to evaluate the formation of 3D spheroids and adipogenic differentiation in vitro, providing a more physiologically relevant system for studying adipose tissue and identifying potential therapeutic targets for obesity and obesity-related diseases.

2. Materials and Methods

2.1. Cell Culture

The murine macrophage cell line J774.1, the murine fibroblast cell line NIH-3T3, and the murine 3T3-L1 pre-adipocytes were obtained from a cell bank in Rio de Janeiro, Brazil. Macrophages and fibroblasts (J771.1 and NIH-3T3) were maintained in Dulbecco's Modified Eagle Medium (DMEM—Sigma®, St. Louis, MO, USA) supplemented with 10% fetal bovine serum (FBS—Gibco®, Grand Island, NY, USA), while pre-adipocytes (3T3-L1) were maintained in DMEM supplemented with 10% calf serum (CS—Gibco®), all containing 100 U/mL of penicillin, 100 µg/mL of streptomycin, and 10 mM of 4-(2-hydroxyethyl)-1-piperazineethanesulfonic acid (HEPES) (Gibco®). Cells were cultured at 37 °C in an atmosphere of 5% CO_2, and the medium was changed every 48 h. The cells were cultured until they reached 80–90% confluence and were then subcultured. 3T3-L1 pre-adipocytes and NIH-3T3 fibroblasts were dissociated with 0.25% trypsin for 5 min at 37 °C, while J774.1 macrophages were detached by scraping with a rubber policeman.

2.2. 3D Cell Culture

In the 3D cell culture, agarose powder (Ludwig Biotecnologia Ltda., Rio Grande do Sul, Brazil) was dissolved in distilled water to a final concentration of 2% (*w*/*v*). The solution was then heated to 60–80 °C until complete dissolution and transferred to a 96-well plate (50 µL/well), followed by 30 min of sterilization under UV light.

2.3. Generation of Mono and Heterospheroids Using the Liquid Overlay Technique and Adipogenic Differentiation Induction

Five spheroid conditions were established based on previous work with modifications [44]. Monospheroids were formed with 3T3-L1 or NIH-3T3, and heterospheroids were produced with a combination of 3T3-L1:J774.1, 3T3-L1:NIH-3T3 or 3T3-L1:J774.1:NIH-3T3 (1:1:1, 1.2×10^4 cell/well). Plates were maintained at 37 °C in an atmosphere of 5% CO_2 and four days after seeding, adipogenic differentiation was induced. The medium was replaced with adipogenic differentiation induction medium (MDI) containing DMEM supplemented with 10% FBS, 500 µM of 3-isobutyl-1-methylxanthine (IBMX), 1 µM dexamethasone (DEX), and 1.67 µM insulin (INS) (all from Sigma®). After 3 days, the induction medium was replaced with maintenance medium containing DMEM supplemented with 10% FBS and 1.67 µM INS, which was replaced every 2 days for a total of 11 days.

Another five spheroid conditions were generated without MDI (DMEM + 10% CS) for the same period, with half of the medium changed every 48 h as a control group. After 11 days of 3D cell culture, the supernatant from both control spheroids and those exposed to MDI was collected and stored at −80 °C.

2.4. Cell Viability Assessment and Sizing

Cell viability was assessed using the Trypan blue exclusion test [45]. Briefly, eight spheroids from each 3D condition were transferred to microtubes, washed with PBS, and dissociated with 0.25% trypsin for 10 min at 37 °C. Subsequently, 1 mL of PBS and 500 µL of FBS were added, followed by centrifugation at 1800× *g* for 5 min. The supernatant was discarded, and the cells were stained with a 0.5% Trypan blue solution (Sigma®) (1:1 *v*/*v* in DMEM) and counted in a Neubauer chamber. Spheroids were photographed using an inverted light microscope equipped with a DCM 510 camera and a 40× objective lens on days 4, 7, and 11. Images were captured using ScopePhoto 3.0 software, and the horizontal diameter was measured using ImageJ Version 1.50 [46].

2.5. Morphology of the Mono and Heterospheroids

External cellular morphology was evaluated by scanning electron microscopy (SEM) as previously described by [47], with modifications. After 11 days of 3D cell culture, spheroids were transferred to microtubes and washed twice with PBS. Subsequently, the spheroids were fixed with 2.5% glutaraldehyde and 4% paraformaldehyde at room temperature for 30 min. Following fixation, the spheroids were incubated in osmium tetroxide for 1 h in the dark, followed by four washes in distilled water. The spheroids were then dehydrated in ethanol diluted in distilled water at increasing concentrations (80%, 90%, 96%, and 100%) and incubated in a mixture of hexamethyldisilane (HMDS) (1:1 in ethanol) for 15 min each. This was followed by two incubations in pure HMDS for 15 min each. Finally, the spheroids were covered with HMDS until complete evaporation. The spheroids were transferred to conductive carbon adhesive tabs, sputtered with gold particles, and analyzed using a scanning electron microscope (SEM, JEOL JSM-6390LV).

2.6. Quantification of Intracellular Lipids

Intracellular lipids were quantified by flow cytometry using the lipophilic stain Nile Red (Sigma®), as previously described [48], with modifications. Spheroids (n = 16) were collected on day 11 and dissociated using 0.25% trypsin for 15 min at 37 °C, followed by centrifugation for 5 min at 1800× *g*. Subsequently, the supernatant was discarded, and the pellet was fixed with 2% formaldehyde at room temperature for 20 min. After that, the cells were washed with PBS and centrifuged again. Nile Red (1 µg/mL) in PBS was added to the cells and incubated at room temperature for 30 min in the dark. Cells were then washed and analyzed using a Flow Cytometer (FACS Canto IITM, BD Biosciences, Franklin Lakes, NJ, USA) with the Flowing 2.5 software (University of Turku) or stained with DAPI (Sigma®) (diluted 1:1000 in PBS) for confocal microscopy (Leica DMI6000 B equipped with

a 20× oil-immersion objective, with excitation parameters of 405 nm for DAPI and 488 nm for Nile Red). The captured images were analyzed using LAS AF Lite software version 3.3.

2.7. Protein Extraction and NO Analysis for Inflammatory Profile

For protein extraction, eight spheroids from each 3D condition were collected, washed with PBS, and dissociated using 0.25% trypsin for 10 min at 37 °C, followed by centrifugation at 1800× *g* for 10 min. Subsequently, protein extraction was performed with 120 µL of RIPA buffer containing 10 mM Tris-HCl (pH 7.5), 150 mM sodium chloride, 1% Triton X-100®, 0.1% sodium dodecyl sulfate, 1 mM phenylmethylsulfonyl fluoride, 5 µg/mL aprotinin, 1 µg/mL leupeptin, and 1 µg/mL pepstatin (all from Sigma®). Protein levels were quantified using the Lowry method [49], with bovine serum albumin as a standard reagent. Nitric oxide (NO) levels were measured in the supernatant of the spheroids used for protein extraction using Griess reagent [50]. The basal release of nitric oxide (NO) was determined in the supernatant from a pool of eight spheroids. The NO results were normalized to the total protein concentration extracted from each 3D condition after 11 days of culture.

2.8. Statistical Analyses

Results are presented as the mean ± standard deviation of duplicate or triplicate tests conducted on alternate days. Statistical analyses were performed using GraphPad Prism 5, and significance was determined with one-way analysis of variance followed by Dunnett's multiple comparisons test or Student's paired *t*-test for comparisons with the control group. Values with $p \leq 0.05$ were considered significantly different.

3. Results

3.1. Macrophages and MDI Medium Influence Cell Growth and Viability on Spheroids

The adipogenic differentiation protocol for the pre-adipocyte lineage was established in a 2D model to validate the MDI for subsequent assays in 3D. For adipogenesis, 3T3-L1 pre-adipocytes were subjected to MDI, and after 7 days, the differentiated cells were stained with Oil Red or Nile Red and visualized under a light and fluorescence microscope, respectively. When exposed to a specific hormonal medium, these cells restart the cell cycle, undergo clonal expansion, and enter the terminal differentiation phase, resulting in changes in morphology and intracellular lipid storage.

In this work, lipid formation was confirmed via visualization in the 2D cell culture, revealing red staining via Oil Red staining (Supplementary Figure S1) and green staining via Nile Red staining (Supplementary Material Table S2). For the 3D experiments, spheroids maintained in control medium were cultured for the same period as those exposed to the adipogenic differentiation medium (Figure 1A). In both groups, spheroids were successfully formed (Figure 1B,C). The size of the spheroids was evaluated on days 4, 7, and 11 by measuring the horizontal diameter of all 3D models. The growth profile of each condition (control and MDI) is shown in Figure 1D,E, respectively (diameters provided in Supplementary Tables S1 and S2).

The results indicated that some of the spheroid models maintained in control medium exhibited a decrease in size in comparison to MDI medium. On the 11th day of culture, the monospheroid formed by the 3T3-L1 lineage exhibited the smallest size, while the heterospheroid established with 3T3-L1 cells was the only one to show significant growth during this period. In comparison to the control group, the MDI-treated group displayed a notable variation in spheroid size. Furthermore, the heterospheroid formed by the combination of 3T3-L1 and J774 cells presented the largest size on the fourth day and remained constant over time, reaching a diameter of 200.6 ± 21.66 µm (Figure 1D,E).

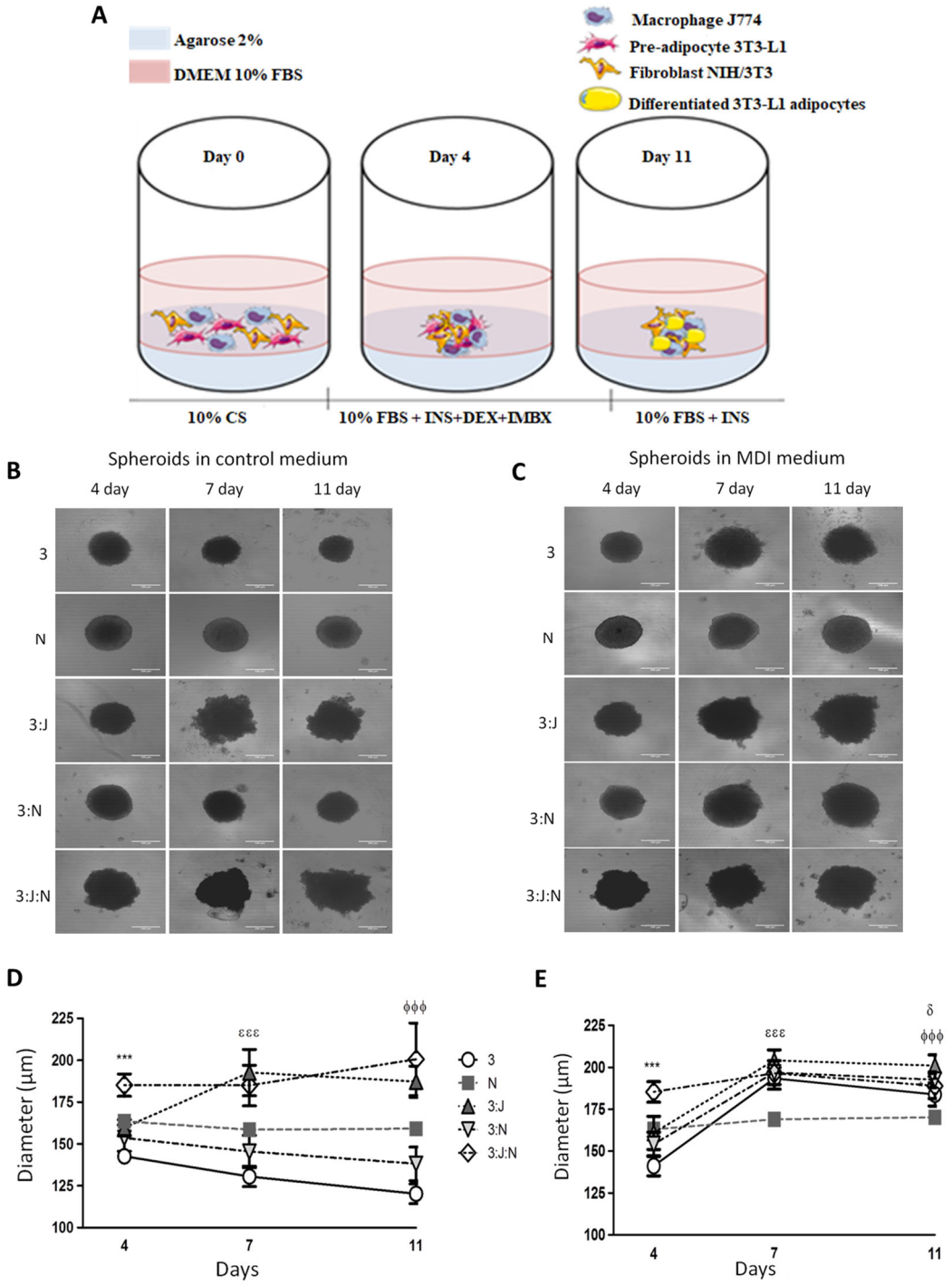

Figure 1. Spheroid growth and cell viability. The model for the spheroid formation process (**A**). Representative images of spheroids formation in control (**B**) and MDI medium (**C**). Scale bar: 100 µm. Data are expressed as the mean ± standard deviation (SD) of three experiments. One-way ANOVA, followed by Dunnett's multiple comparisons test, was used for statistical significance. Growth of spheroids formed on control medium (**D**). *** ($p < 0.001$) 3:J:N group in relation to all other groups on day 4. єєє ($p < 0.001$) 3:J:N group in relation to all other groups except 3:J on day 7. ϕϕϕ ($p < 0.001$) 3:J:N group in relation to all other groups except 3:J on day 11. Growth of spheroids formed on MDI medium (**E**). *** ($p < 0.001$) 3:J:N group in relation to all other groups on day 4. єєє ($p < 0.001$) 3:J:N group in relation to N group on day 7. ϕϕϕ ($p < 0.001$) 3:J:N group in relation to N group on day 11. δ ($p < 0.05$) 3:J:N group in relation to 3:J group on day 11. Legend: 3 = 3T3-L1; N = NIH-3T3; 3:J = 3T3-L1:J774; 3:N = 3T3-L1:NIH-3T3; 3:J:N = 3T3-L1:J774:NIH-3T3.

The diameter of the spheroids subjected to MDI (Figure 1) indicates that these models exhibited an increase in size when exposed to the hormonal medium. The heterospheroid 3:J had the largest diameter on day 4; however, by day 7, all other models showed similar sizes, except for the NIH/3T3 (N) monospheroid, which was the only model that did not exhibit any increase in size when exposed to MDI. Moreover, the viability of the cells was evaluated on day 11 and was around 70–80%. The MDI appeared to improve this viability, with no significant difference between groups (Table 1).

Table 1. Cell viability after 11 days of 3D culture.

	Viability (%)	
	Control	**MDI**
3	80.63 ± 4.7	81.55 ± 6.1
N	92.85 ± 3.9	94.56 ± 3.2
3:J	66.76 ± 7.6	79.78 ± 4.4
3:N	87.95 ± 9.3	87.26 ± 4.4
3:J:N	76.87 ± 15.1	84.49 ± 8.3

The external cellular morphology of spheroids was evaluated by SEM, and the images revealed differences between the control group and the MDI group (Figure 2A,B).

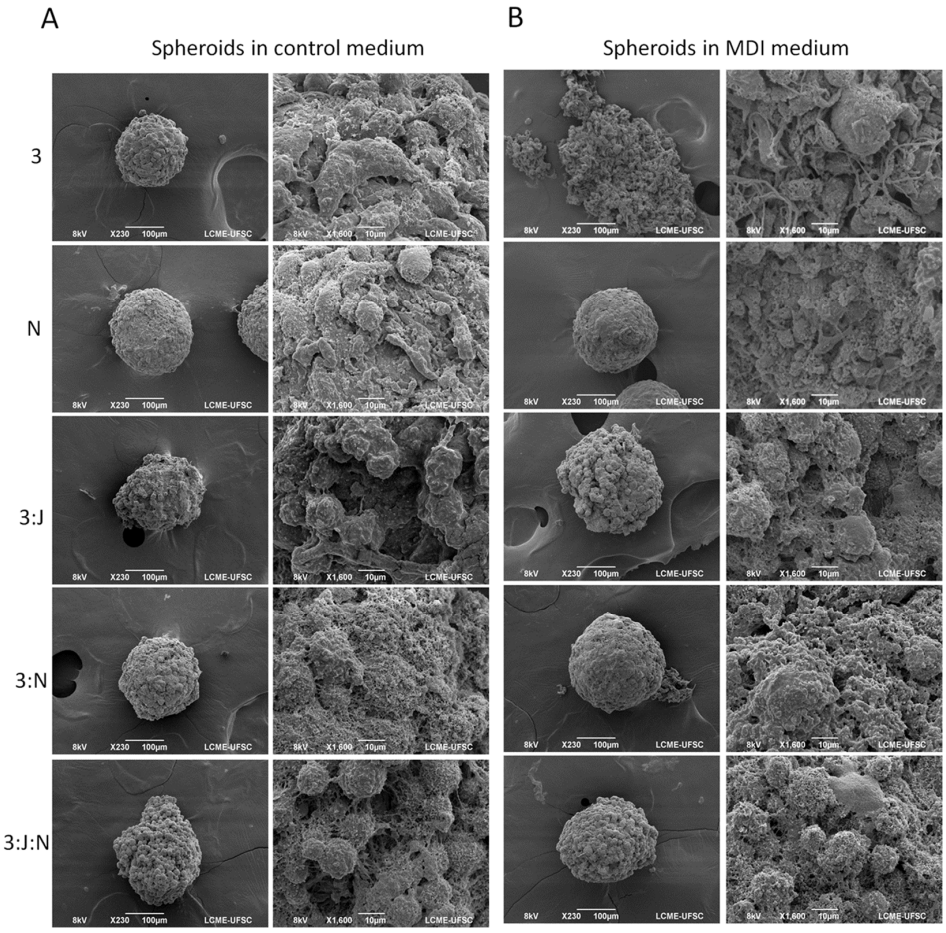

Figure 2. External morphology and cellular viability of different spheroids formed on day 11. SEM-imagens of spheroids formed in control (**A**) and MDI medium (**B**). Scale bar 100 and 10 µm. Legend: 3 = 3T3-L1; N = NIH-3T3; 3:J = 3T3-L1:J774; 3:N = 3T3-L1:NIH-3T3; 3:J:N = 3T3-L1:J774:NIH-3T3.

Regarding phase-contrast images, spheroids cultivated in control medium exhibited a reduction in size on day 11. Additionally, at high magnification, they displayed a rough

surface with the presence of abnormal cells in some conditions. However, cells with a round morphology were also visible, along with cell-to-cell interactions and intense production of the extracellular matrix.

3.2. Spheroids Themselves Induce Adipogenic Differentiation

Adipogenic differentiation was visualized by confocal microscopy (Figure 3A,B) and quantified using flow cytometry (Figure 3C). The results demonstrated that spheroids formed in control medium underwent spontaneous adipogenic differentiation without the need for hormonal stimuli, as shown by Nile Red staining. Importantly, no significant difference in adipogenic differentiation was observed between the control and MDI-treated spheroids for the 3:J condition (control: 75.7 ± 1.7% versus MDI: 60.7 ± 10.3%), indicating that both conditions—control and MDI—produced similar levels of differentiation.

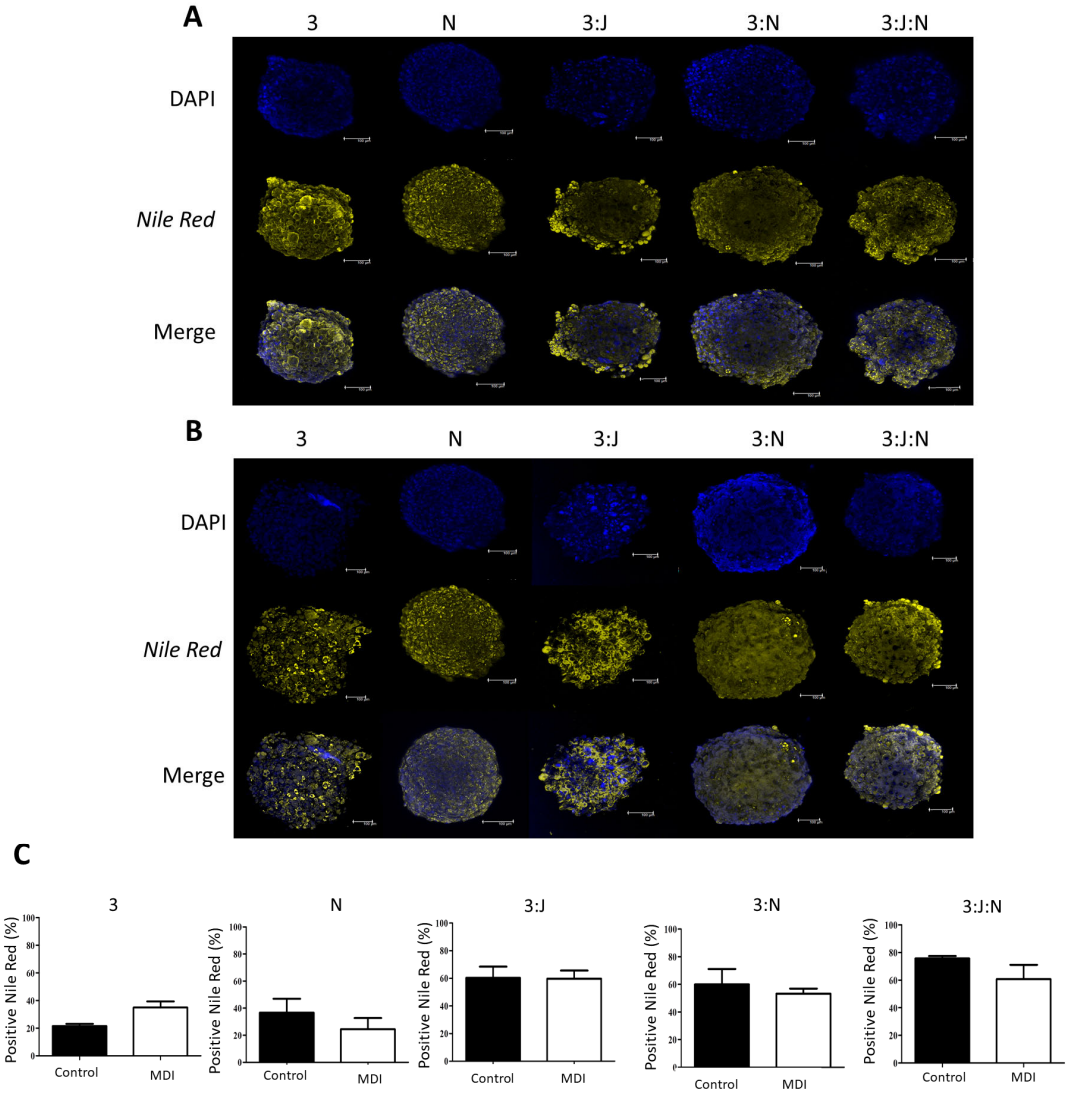

Figure 3. Adipogenic differentiation of mono and heterospheroids with or without hormonal stimuli. Maximum intensity projection from 1 µm apart of spheroids formed in control (**A**) and MDI medium (**B**). Spheroids were stained with Nile red (yellow), and nuclei were counterstained with DAPI (blue). Scale bar 100 µm. Graphic representation of the percentage of positive Nile red cells (**C**). Data are expressed as mean ± SD of three experiments. Statistical analyses by Student's *t*-test. Legend: 3 = 3T3-L1; N = NIH-3T3; 3:J = 3T3-L1:J774; 3:N = 3T3-L1:NIH-3T3; 3:J:N = 3T3-L1:J774:NIH-3T3.

Analyses of the inflammatory profile were conducted on day 11 in the supernatant of spheroids with or without hormonal induction (Figure 4). The results of basal ·NO production were normalized by the total protein content on the same day. As observed in Figure 4, the heterospheroid 3:J:N exhibited the highest production of ·NO, with no significant difference between control and MDI spheroids reported (1.43 ± 0.55 versus 1.49 ± 0.09 µM/µg of protein, respectively). The data presented demonstrate that compared to models 3:J and N, there is sufficient evidence to conclude that the observed effect in the study is statistically significant. This difference is attributed to the composition of the spheroids exposed to MDI.

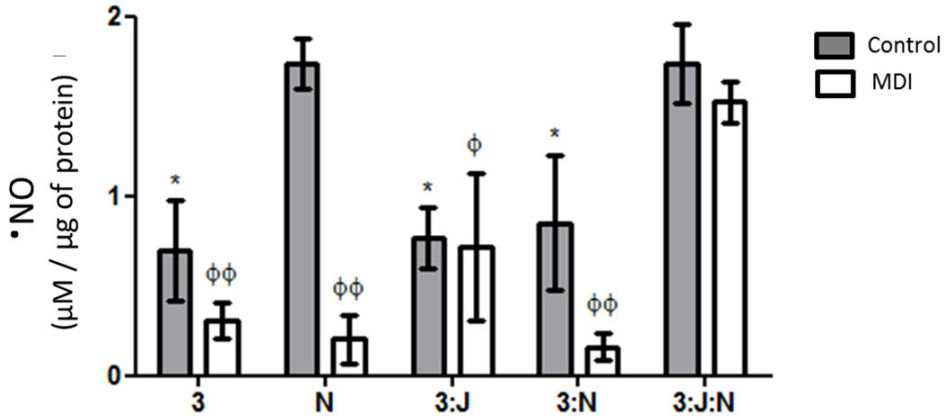

Figure 4. ·NO release profile in the supernatant of spheroids maintained in control medium or treated with MDI. Data are presented as mean ± standard deviation (n = 3). Statistical analysis was performed using one-way ANOVA followed by Bonferroni post hoc test. * ($p < 0.05$) compared to the 3:J model; α ($p < 0.05$) compared to the 3 model; β ($p < 0.05$) compared to the N model; ϕ ($p < 0.05$), ϕϕ ($p < 0.01$) compared to the 3:J. 3 = 3T3-L1; N = NIH/3T3; 3:J = 3T3-L1; 3:N = 3T3-L1/3T3; 3:J:N = 3T3-L1:J774/3T3 model.

4. Discussion

In this study, we developed and characterized an in vitro 3D multicellular spheroid model composed of murine immortalized pre-adipocytes, macrophages, and fibroblasts. This model, which uses easily obtainable and culturable murine cell lines, offers a superior alternative to traditional 2D cultures, as it does not require a differentiation medium. It more accurately mimics in vivo adipose tissue by benefiting from the interconnections and interactions between the cell types, which allow for the spontaneous differentiation of pre-adipocytes. This self-differentiation highlights the potential of the 3D model to replicate key aspects of adipose tissue biology, providing a more physiologically relevant system for studying adipocyte behavior and interactions. The method for generating the spheroids was adapted from a 3D approach previously established in our research group [51]. Spheroids were created using the liquid-overlay technique (LOT) in a 96-well plate coated with agarose gel. LOT is a widely recognized and standardized method [52,53], frequently employed for various purposes [47]. The agarose gel forms a semi-solid, non-adherent surface, making it an ideal substrate for the formation of 3D spheroids. However, the concentration and volume of agarose must be adjusted depending on the specific cell type used [37]. Here, we developed five distinct 3D spheroid models using murine cell lines native to adipose tissue: preadipocytes (3T3-L1), macrophages (J774.1), and fibroblasts (NIH-3T3). The conditions included monospheroids composed of either 3T3-L1 or NIH-3T3 cells, as well as heterospheroids combining 3T3-L1 + J774, 3T3-L1 + NIH-3T3, and 3T3-L1 + J774 + NIH-3T3. Additionally, the spheroids were exposed to adipogenic differentiation medium (MDI) and compared to those maintained in control medium. In all conditions, the spheroids were homogenous in both diameter and shape (Figure 1B,C).

All spheroids cultured in control medium, except those containing macrophages, exhibited smaller diameters compared to the 3 spheroids (Figure 1B). Furthermore, spheroids

treated with MDI showed an increase in size from day 4 to day 7. The only exception was the monospheroid composed of NIH-3T3 cells in MDI, which maintained a consistent size over time (Figure 1C). Previous 3D studies using 3T3-L1 cells demonstrated an increase in size when spheroids were exposed to MDI [36,41]. Additionally, both 3T3-L1 and NIH-3T3 cells exhibited contact inhibition when not exposed to the hormonal medium [54]. According to Stephan and colleagues [55], the availability of serum and glucose in the 3D environment can influence cell proliferation and survival. The increased size of MDI-treated spheroids may be due to media supplementation (insulin and serum), providing an additional growth stimulus, which could also affect cell viability (Table 1). Moreover, we observed that in the presence of macrophages, spheroid size remained stable, highlighting the critical role these cells play in supporting growth and maintaining the 3D model when co-cultured with fibroblasts. Also, the addition of those fibroblasts and macrophage cells are essential to sustaining the spheroid formation and growth [54].

Cell viability is influenced by spheroid size. Large spheroids (>200–300 µm in diameter) tend to exhibit a necrotic core, which can result from reduced nutrient diffusion, insufficient oxygen supply, waste accumulation, and subsequent hypoxia [56–58]. It should be noted that the average spheroid size was limited to approximately 200 µm, with control spheroids showing a mean viability of 71% and MDI-treated spheroids showing 81%. Similar viability rates were reported by Amann and colleagues [59]. In general, the adipogenic differentiation medium seems to have a slight influence on cell viability. However, the control 3:J spheroid showed a significant increase in viability when exposed to the hormonal medium (59.05% vs. 79.36%, respectively).

It has been reported that pre-adipocytes and fibroblasts produce extracellular matrix (ECM) components such as collagen and fibronectin [59,60], which, in addition to contributing to spheroid compaction, promote a smooth surface. In this study, SEM images revealed differences in size between the control and MDI groups, as well as intense cell–cell contact (Figure 2A,B, respectively). Furthermore, except for the NIH-3T3 monospheroid, which displayed a smooth surface, all other conditions exhibited a rough surface. In some cases, such as the control 3:J heterospheroid and the MDI-treated 3T3-L1 monospheroid, individual cells connected by ECM-like structures were observed. These structures have been previously described as a form of communication between cells [61].

Interestingly, according to the results obtained through confocal microscopy and flow cytometry (Figure 3A,C), spheroids formed in control medium also exhibited adipogenic differentiation, suggesting that 3D cell culture can induce self-differentiation, which is more pronounced in co-culture conditions. Ruehl and colleagues [62] revealed that collagen XIV, a component of the ECM expressed in differentiated tissues, can promote pre-adipocyte differentiation.

Although this study did not specifically evaluate the ECM components produced by the cell lineages used in the 3D system, it can be suggested that the intense cell–cell and cell-matrix interactions may have induced the self-differentiation observed in control spheroids. Additionally, co-culture systems containing adipose tissue macrophages and adipose stem cells have been shown to induce the formation of new pre-adipocytes, which display intracellular lipid accumulation and adipogenic gene expression [63]. Furthermore, the study demonstrated that pre-adipocytes formed after co-culture may partly originate from adipose tissue macrophages. A limitation of this study is the use of a fixed 1:1:1 ratio of pre-adipocytes, fibroblasts, and macrophages in the heterospheroids. The effects of varying these cell proportions on spheroid growth and differentiation remain unexplored and could be an important direction for future research. Additionally, while immortalized murine cell lines offer ease of acquisition and culture, they may not fully capture the complexity of in vivo adipose tissue. These findings suggest that paracrine cross-talk between macrophages and other cellular components plays a role in the self-differentiation observed under control conditions.

The inflammatory profile was evaluated through $^{\cdot}$NO production, and the results suggest that the adipogenic differentiation process observed in both control and MDI

conditions contributes to the formation of a 3D multicellular adipose tissue model with an inflammatory profile. While some studies report that the interaction between macrophages and adipocytes increases ·NO synthesis, leading to inhibition of insulin signaling and glucose uptake [64,65], other studies suggest that ·NO can stimulate glucose transport via a mechanism independent of insulin signaling [66]. In this study, the 3D multicellular adipose tissue model exhibited adipogenic differentiation under both conditions (control and MDI), even in the presence of an inflammatory profile.

5. Conclusions

This study demonstrated that the 3D multicellular adipose tissue model exhibited adipogenic differentiation under both conditions (control and MDI), even in the presence of an inflammatory profile. In conclusion, the development of new methods and in vitro models of adipose tissue can be valuable tools for basic research and drug screening. The 3D multicellular in vitro model established here offers a more advanced platform for understanding the mechanisms involved in adipogenesis, tissue engineering, and the evaluation of therapeutic responses in obesity treatment.

Supplementary Materials: The following supporting information can be downloaded at https://www.mdpi.com/article/10.3390/organoids3040018/s1. Figure S1. Adipogenic differentiation of the 3T3-L1 cell line. Table S1. Diameter of spheroids in control medium; Table S2: Diameter of spheroids in MDI medium.

Author Contributions: T.D.-M. devised and planned the experimental design under the guidance of F.B.F.-M., T.D.-M., N.A.S., M.L.C.B. and M.P.R. conducted the experiments and analyzed the data, while A.H.S. and L.S.A. contributed to the methodology. T.D.-M., M.L.C.B. and V.P.G.M. wrote the manuscript, and T.B.C.-P. and F.B.F.-M. supervised the project. All authors contributed to the critical evaluation of the intellectual content. All authors have read and agreed to the published version of the manuscript.

Funding: The research was supported by CAPES (Coordenação de Aperfeiçoamento de Pessoal de Nível Superior) scholarship and the Fundação de Amparo à Pesquisa e Inovação do Estado de Santa Catarina (FAPESC—3655/2013).

Institutional Review Board Statement: Not applicable.

Informed Consent Statement: Not applicable.

Data Availability Statement: The data underlying this article are available in the article and its online Supplementary Material. If further details are required, this information may be shared upon reasonable request to the corresponding author.

Acknowledgments: The authors would like to thank the LCME-2024 (Central Laboratory of Electron Microscopy) for technical support and LAMEB (Multiuser Laboratory of Biology Studies) both at UFSC.

Conflicts of Interest: The authors declare no conflicts of interest.

References

1. WHO. The Global Health Observatory. 2024. Available online: https://www.who.int/data/gho/indicator-metadata-registry/imr-details/3420 (accessed on 19 August 2024).
2. Muniesa-González, P.; González-Mártinez, M.; Hu, F.B.; Després, J.P.; Matsuzawa, Y.; Loos, R.J.F.; Moreno, L.A.; Bray, G.A.; Martinez, J.A. Obesity. *Nat. Rev. Dis. Prim.* **2017**, *3*, 1–18.
3. Chait, A.; den Hartigh, L.J. Adipose Tissue Distribution, Inflammation and Its Metabolic Consequences, Including Diabetes and Cardiovascular Disease. *Front. Cardiovasc. Med.* **2020**, *7*, 22. [CrossRef] [PubMed]
4. Haylett, W.L.; Ferris, W.F. Adipocyte–progenitor cell communication that influences adipogenesis. *Cell. Mol. Life Sci.* **2020**, *77*, 115–128. [CrossRef] [PubMed]
5. Yang, L.; Shu-Wen, Q.; Yan, T.; Qi-Qun, T. The secretory function of adipose tissues in metabolic regulation. *Life Metabolism* **2024**, *3*, loae003.

6. Clemente-Suárez, V.J.; Redondo-Flórez, L.; Beltrán-Velasco, A.I.; Martín-Rodríguez, A.; Martínez-Guardado, I.; Navarro-Jiménez, E.; Laborde-Cárdenas, C.C.; Tornero-Aguilera, J.F. The Role of Adipokines in Health and Disease. *Biomedicines* **2023**, *11*, 1290. [CrossRef]
7. Ouchi, N.; Parker, J.L.; Lugus, J.J.; Walsh, K. Adipokines in inflammation and metabolic disease. *Immunology* **2011**, *11*, 85–97. [CrossRef]
8. Avram, M.M.; Avram, A.S.; James, W.D. Subcutaneous fat in normal and diseased states 3. Adipogenesis: From stem cell to fat cell. *Am. Acad. Dermatol.* **2007**, *56*, 472–492. [CrossRef]
9. Sun, K.; Kusminski, C.C.M.; Scherer, P.E.P. Adipose tissue remodeling and obesity. *J. Clin. Investig.* **2011**, *121*, 2094–2101. [CrossRef]
10. Esteve Ràfols, M. Adipose tissue: Cell heterogeneity and functional diversity. *Endocrinol. Y Nutr.* **2014**, *61*, 100–112. [CrossRef]
11. Huang, B.; Yuan, H.D.; Kim, D.Y.; Quan, H.Y.; Chung, S.H. Cinnamaldehyde prevents adipocyte differentiation and adipogenesis via regulation of peroxisome proliferator-activated receptor-γ (PPARγ) and AMP-activated protein kinase (AMPK) pathways. *J. Agric Food Chem.* **2011**, *59*, 3666–3673. [CrossRef]
12. Guru, A.; Issac, P.K.; Velayutham, M.; Saraswathi, N.T.; Arshad, A.; Arockiaraj, J. Molecular mechanism of down-regulating adipogenic transcription factors in 3T3-L1 adipocyte cells by bioactive anti-adipogenic compounds. *Mol. Biol. Rep.* **2021**, *48*, 743–761. [CrossRef] [PubMed]
13. Ceppo, F.; Berthou, F.; Jager, J.; Dumas, K.; Cormont, M.; Tanti, J.F. Implication of the Tpl2 kinase in inflammatory changes and insulin resistance induced by the interaction between adipocytes and macrophages. *Endocrinology* **2014**, *155*, 951–964. [CrossRef] [PubMed]
14. Moon, H.-S.; Chung, C.-S.; Lee, H.-G.; Kim, T.-G.; Choi, Y.-J.; Cho, C.-S. Inhibitory effect of (-)-epigallocatechin-3-gallate on lipid accumulation of 3T3-L1 cells. *Obesity* **2007**, *15*, 2571–2582. [CrossRef] [PubMed]
15. Filippin-Monteiro, F.B.; Oliveira EM de Sandri, S.; Knebel, F.H.; Albuquerque, R.C.; Campa, A. Serum amyloid A is a growth factor for 3T3-L1 adipocytes, inhibits differentiation and promotes insulin resistance. *Int. J. Obes.* **2012**, *36*, 1032–1039. [CrossRef]
16. Guo, W.; Zhang, K.-M.; Tu, K.; Li, Y.-X.; Zhu, L.; Xiao, H.-S.; Yang, Y.; Wu, J.-R. Adipogenesis licensing and execution are disparately linked to cell proliferation. *Cell Res.* **2009**, *19*, 216–223. [CrossRef]
17. Green, H.; Meuth, M. An established pre-adipose cell line and it's differentation in culture. *Cell* **1975**, *5*, 19–27. [CrossRef]
18. Farmer, S.R. Transcriptional control of adipocyte formation. *Cell Metab.* **2006**, *4*, 263–273. [CrossRef]
19. Mehra, A.; Macdonald, I.; Pillay, T.S. Variability in 3T3-L1 adipocyte differentiation depending on cell culture dish. *Anal. Biochem.* **2007**, *362*, 281–283. [CrossRef]
20. Kang, M.; Kang, N.; Ko, S.; Kim, Y.; Jeon, Y. Anti-obesity effects of seaweeds of Jeju Island on the differentiation of 3T3-L1 preadipocytes and obese mice fed a high-fat diet. *Food Chem. Toxicol.* **2016**, *90*, 36–44. [CrossRef]
21. Mukhtar, F.; Stieglitz, K.; Ali, S.; Ejaz, A.; Choudhary, M.I.; Fakhri, M.I.; Fakhri, M.I.; Salar, U.; Khan, K.M. Coumarin and Biscoumarin Inhibit in Vitro Obesity Model. *Adv. Biol. Chemestry* **2016**, *6*, 152–168. [CrossRef]
22. Seo, Y.-S.; Kang, O.-H.; Kim, S.-B.; Mun, S.-H.; Kang, D.-H.; Yang, D.-W.; Choi, J.-G.; Lee, Y.-M.; Kang, D.-K.; Lee, H.-S.; et al. Quercetin prevents adipogenesis by regulation of transcriptional factors and lipases in OP9 cells. *Int. J. Mol. Med.* **2015**, *35*, 1779–1785.
23. Balaban, S.; Shearer, R.F.; Lee, L.S.; Van Geldermalsen, M.; Schreuder, M.; Shtein, H.C.; Cairns, R.; Thomas, K.C.; Fazakerley, D.J.; Grewal, T.; et al. Adipocyte lipolysis links obesity to breast cancer growth: Adipocyte-derived fatty acids drive breast cancer cell proliferation and migration. *Cancer Metab.* **2017**, *5*, 1–14. [CrossRef]
24. Lo, K.A.; Labadorf, A.; Kennedy, N.J.; Han, M.S.; Sing, Y.; Matthews, B.; Xin, X.; Sun, L.; Davis, R.J.; Lodish, H.F.; et al. Analysis of in vitro insulin resistance models and their physiological relevance to in vivo diet-induced adipose insulin resistance. *Cell Rep.* **2013**, *5*, 259–270. [CrossRef]
25. Abdesselem, H.; Madani, A.; Hani, A.; Al-Noubi, M.; Goswami, N.; Ben Hamidane, H.; Billing, A.M.; Pasquier, J.; Bonkowski, M.S.; Halabi, N.; et al. SIRT1 limits adipocyte hyperplasia through c-Myc inhibition. *J. Biol. Chem.* **2016**, *291*, 2119–2135. [CrossRef]
26. Ma, X.; Ding, W.; Wang, J.; Wu, G.; Zhang, H.; Yin, J.; Zhou, L.; Li, D. LOC66273 Isoform 2, a Novel Protein Highly Expressed in White Adipose Tissue, Induces Adipogeneses in 3T3-L1 Cells. *J. Nutr.* **2012**, *142*, 448–455. [CrossRef]
27. Som, D.; Choi, H.; Soo, B.; Kon, W.; Chul, S.; Oh, K.; Bae, K.H. c-Jun regulates adipocyte differentiation via the KLF15-mediated mode. *Biochem. Biophys. Res. Commun.* **2016**, *469*, 552–558.
28. Xu, Y.; Du, J.; Zhang, P.; Zhao, X.; Li, Q.; Jiang, A.; Jiang, D.; Tang, G.; Jiang, Y.; Wang, J.; et al. MicroRNA-125a-5p Mediates 3T3-L1 Preadipocyte Proliferation and Differentiation. *Molecules* **2018**, *23*, 317. [CrossRef] [PubMed] [PubMed Central]
29. Wang, Y.; Zhang, J.; Chu, X.; Wang, M.; Xin, Y.; Liu, S. MiR-146a-5p, targeting ErbB4, promotes 3T3-L1 preadipocyte differentiation through the ERK1/2/PPAR-γ signaling pathway. *Lipids Health Dis.* **2022**, *21*, 54. [CrossRef] [PubMed] [PubMed Central]
30. Xu, J.; Zhang, L.; Shu, G.; Wang, B. microRNA-16-5p promotes 3T3-L1 adipocyte differentiation through regulating EPT1. *Biochem. Biophys. Res. Commun.* **2019**, *514*, 1251–1256. [CrossRef]
31. Subramaniyan, S.A.; Kim, S.; Hwang, I. Cell-Cell Communication Between Fibroblast and 3T3-L1 Cells Under Co-culturing in Oxidative Stress Condition Induced by H_2O_2. *Appl. Biochem. Biotechnol.* **2016**, *180*, 668–681. [CrossRef]
32. Suganami, T.; Tanimoto-Koyama, K.; Nishida, J.; Itoh, M.; Yuan, X.; Mizuarai, S.; Kotani, H.; Yamaoka, S.; Miyake, K.; Aoe, S.; et al. Role of the Toll-like receptor 4/NF-kB pathway in saturated fatty acid-induced inflammatory changes in the interaction between adipocytes and macrophages. *Arterioscler. Thromb. Vasc. Biol.* **2007**, *27*, 84–91. [CrossRef] [PubMed]

33. Egeblad, M.; Nakasone, E.S.; Werb, Z. Tumors as Organs: Complex Tissues That Interface with the Entire Organism. *Dev. Cell.* **2010**, *18*, 884–901. [CrossRef]
34. Imamura, Y.; Mukohara, T.; Shimono, Y.; Funakoshi, Y. Comparison of 2D- and 3D-culture models as drug-testing platforms in breast cancer. *Oncol. Rep.* **2015**, *33*, 1837–1843. [CrossRef]
35. Daquinag, A.C.; Souza, G.R.; Kolonin, M.G. Adipose tissue engineering in three-dimensional levitation tissue culture system based on magnetic nanoparticles. *Tissue Eng. Part C Methods* **2013**, *19*, 336–344. [CrossRef]
36. Habanjar, O.; Diab-Assaf, M.; Caldefie-Chezet, F.; Delort, L. 3D Cell Culture Systems: Tumor Application, Advantages, and Disadvantages. *Int. J. Mol. Sci.* **2021**, *22*, 12200. [CrossRef] [PubMed] [PubMed Central]
37. Ravi, M.; Paramesh, V.; Kaviya, S.R.; Anuradha, E.; Paul Solomon, F.D. 3D cell culture systems: Advantages and applications. *J. Cell. Physiol.* **2015**, *230*, 16–26. [CrossRef]
38. Achilli, T.-M.; Meyer, J.; Morgan, J.R. Advances in the formation, use and understanding of multi- cellular spheroids. *Expert Opin. Biol. Ther.* **2012**, *12*, 1347–1360. [CrossRef]
39. Wen, Z.; Liao, Q.; Hu, Y.; You, L.; Zhou, L.; Zhao, Y. A spheroid-based 3-D culture model for pancreatic cancer drug testing, using the acid phosphatase assay. *Brazilian J. Med. Biol. Res.* **2013**, *46*, 634–642. [CrossRef]
40. Turner, P.A.; Harris, L.M.; Purser, C.A.; Baker, R.C.; Janorkar, A.V. A surface-tethered spheroid model for functional evaluation of 3T3-L1 adipocytes. *Biotechnol. Bioeng.* **2014**, *111*, 174–183. [CrossRef]
41. Turner, P.A.; Tang, Y.; Weiss, S.J.; Janorkar, A.V. Three-Dimensional Spheroid Cell Model. *Tissue Eng.* **2015**, *21*, 1837–1847. [CrossRef]
42. Fischbach, C.; Seufert, J.; Staiger, H.; Hacker, M.; Neubauer, M.; Göpferich, A.; Blunk, T. Three-dimensional in vitro model of adipogenesis: Comparison of culture conditions. *Tissue Eng.* **2004**, *10*, 215–229. [CrossRef] [PubMed]
43. Daya, S.; Loughlin, A.J.; MacQueen, H.A. Culture and differentiation of preadipocytes in two-dimensional and three-dimensional in vitro systems. *Differentiation* **2007**, *75*, 360–370. [CrossRef] [PubMed]
44. Saleh, N.A.; Rode, M.P.; Sierra, J.A.; Silva, A.H.; Miyake, J.A.; Filippin-Monteiro, F.B.; Creczynski-Pasa, T.B. Three-dimensional multicellular cell culture for anti-melanoma drug screening: Focus on tumor microenvironment. *Cytotechnology* **2021**, *73*, 35–48. [CrossRef]
45. Strober, W. Trypan blue exclusion test of cell viability. *Curr. Protoc. Immunol.* **2001**, *111*, A3.B.1–A3.B.3.
46. Schneider, C.A.; Rasband, W.S.; Eliceiri, K.W. NIH Image to ImageJ: 25 years of image analysis. *Nat. Methods* **2012**, *9*, 671–675. [CrossRef]
47. Dorst, N.; Oberringer, M.; Grässer, U.; Pohlemann, T.; Metzger, W. Analysis of cellular composition of co-culture spheroids. *Ann. Anat.* **2014**, *196*, 303–311. [CrossRef]
48. Su, S.-H.; Shyu, H.-W.; Yeh, Y.-T.; Chen, K.-M.; Yeh, H.; Su, S.-J. Caffeine inhibits adipogenic differentiation of primary adipose-derived stem cells and bone marrow stromal cells. *Toxicol. Vitr.* **2013**, *27*, 1830–1837. [CrossRef]
49. Lowry, O.H.; Rosebrough, N.J.; Farr, A.L.; Randall, R.J. Protein measurement with the folin phenol reagent. *J. Biol. Chem.* **1951**, *193*, 265–275. [CrossRef]
50. Griess, P. Bemerkungen zu der Abhandlung der HH. Weselsky und Benedikt "Ueber einige Azoverbindungen". *Berichte der Dtsch. Chem. Gesellschaft.* **1879**, *12*, 426–428. [CrossRef]
51. Turner, P.A.; Gurumurthy, B.; Bailey, J.L.; Elks, C.M.; Janorkar, A.V. Adipogenic differentiation of human adipose-derived stem cells grown as spheroids. *Process Biochem.* **2017**, *59*, 312–320. [CrossRef]
52. Yuhas, J.M.; Li, A.P.; Martinez, A.; Ladman, A.J. A Simplified Method for Production and Growth of Multicellular Tumor Spheroids. *Cancer Res.* **1977**, *37*, 3639–3643. [PubMed]
53. Carlsson, J.; Yuhas, J.M. Liquid-overlay culture of cellular spheroids. *Recent Results Cancer Res.* **1984**, *95*, 1–23. [PubMed]
54. Rama-Esendagli, D.; Esendagli, G.; Yilmaz, G.; Guc, D. Spheroid formation and invasion capacity are differentially influenced by co-cultures of fibroblast and macrophage cells in breast cancer. *Mol. Biol. Rep.* **2014**, *41*, 2885–2892. [CrossRef] [PubMed]
55. Stephan, S.; Johnson, W.E.; Roberts, S. The influence of nutrient supply and cell density on the growth and survival of intervertebral disc cells in 3D culture. *Eur. Cell. Mater.* **2011**, *22*, 97–108. [CrossRef]
56. Cui, X.; Hartanto, Y.; Zhang, H. Advances in multicellular spheroids formation. *J. R. Soc. Interface.* **2017**, *14*, 2–15. [CrossRef]
57. Hamilton, G. Multicellular spheroids as an in vitro tumor model. *Cancer Latters* **1998**, *131*, 29–34. [CrossRef]
58. Mueller-Klieser, W.; Freyer, J.P.; Sutherland, R.M. Influence of glucose and oxygen supply conditions oxygenation of multicellular spheroids. *Br. J. Cancer* **1986**, *53*, 345–353. [CrossRef]
59. Amann, A.; Zwierzina, M.; Gamerith, G.; Bitsche, M.; Huber, J.M.; Vogel, G.F.; Blumer, M.; Koeck, S.; Pechriggl, E.J.; Kelm, J.M.; et al. Development of an innovative 3D cell culture system to study tumour—Stroma interactions in non-small cell lung cancer cells. *PLoS ONE* **2014**, *9*, e92511. [CrossRef]
60. Kuri-Harcuch, W.; Arguello, C.; Marsch-Moreno, M. Extracellular matrix production by mouse 3T3-F442A cells during adipose differentiation in culture. *Differentiation* **1984**, *28*, 173–178. [CrossRef]
61. Ware, M.J.; Colbert, K.; Keshishian, V.; Ho, J.; Corr, S.J.; Curley, S.A.; Godin, B. Generation of Homogenous Three-Dimensional Pancreatic Cancer Cell Spheroids Using an Improved Hanging Drop Technique. *Tissue Eng. Part C Methods* **2016**, *22*, 312–321. [CrossRef]

62. Ruehl, M.; Erben, U.; Schuppan, D.; Wagner, C.; Zeller, A.; Freise, C.; Al-Hasani, H.; Loesekann, M.; Notter, M.; Wittig, B.M.; et al. The Elongated First Fibronectin Type III Domain of Collagen XIV Is an Inducer of Quiescence and Differentiation in Fibroblasts and Preadipocytes. *J. Biol. Chem.* **2005**, *280*, 38537–38543. [CrossRef] [PubMed]
63. Chazenbalk, G.; Berlotto, C.; Heneidi, S.; Jumabay, M.; Trivax, B.; Aronowitz, J.; Yoshimura, K.; Simmons, C.F.; Dumesic, D.A.; Azziz, R. Novel Pathway of Adipogenesis through Cross-Talk between Adipose Tissue Macrophages, Adipose Stem Cells and Adipocytes: Evidence of Cell Plasticity. *PLoS ONE* **2011**, *6*, e17834. [CrossRef] [PubMed]
64. Fite, A.; Abou-Samra, A.B.; Seyoum, B. Macrophages Inhibit Insulin Signalling in Adipocytes: Role of Inducible Nitric Oxide Synthase and Nitric Oxide. *Can. J. Diabetes* **2015**, *39*, 36–43. [CrossRef] [PubMed]
65. Xie, L.; Ortega, M.T.; Mora, S.; Chapes, S.K. Interactive Changes between Macrophages and Adipocytes. *Clin. Vaccine Immunol.* **2010**, *17*, 651–659. [CrossRef]
66. Tanaka, T.; Nakatani, K.; Morioka, K.; Urakawa, H.; Maruyama, N.; Kitagawa, N.; Katsuki, A.; Araki-Sasaki, R.; Hori, Y.; Gabazza, E.; et al. Nitric oxide stimulates glucose transport through insulin-independent GLUT4 translocation in 3T3-L1 adipocytes. *Eur. J. Endocrinol.* **2003**, *149*, 61–67. [CrossRef]